DALTON
FULL PAPER

Substitution of bridging S_2 ligands in the $[Nb_2(\mu\text{-}S_2)_2]^{4+}$ core: a simple route to $[Nb_2(Se_2)_2]^{4+}$, $[Nb_2(S)(Te_2)]^{4+}$ and $[Nb_2(S)_2]^{4+}$

Maxim Sokolov,[*a,b] **Hideo Imoto,**[a] **Taro Saito**[a] **and Vladimir Fedorov**[b]

[a] *Department of Chemistry, School of Science, The University of Tokyo, Hongo, Bunkyo-ku, Tokyo 113-0333, Japan*
[b] *Institute of Inorganic Chemistry of the Russian Academy of Sciences, pr. Lavrentyeva 3, 630090, Novosibirsk, Russia*

Received 24th August 1998, Accepted 3rd November 1998

Reactions of $[Nb_2(\mu\text{-}S_2)_2(dtc)_4]$ **1** (dtc = diethyldithiocarbamate, S_2CNEt_2) with chalcogen-transfer reagents PEt_3Y (Y = Se or Te) were investigated. With PEt_3Se, fully substituted $[Nb_2(\mu\text{-}Se_2)_2(dtc)_4]$ **2** forms if a catalytic amount of free PEt_3 is present. However PEt_3Te gives $[Nb_2(S)(Te_2)(dtc)_4]$ **3** which has a new core with two different chalcogens acting as bridges. The structures of both **2** and **3** were determined by X-ray analysis [**2**: Nb–Nb 2.974(2), Se–Se 2.303(2). **3**: Nb–Nb 2.920(4), Te–Te 2.648(3) Å]. Electrochemistry of **2** and **3** was studied and a reversible one-electron oxidation was found for **2**, giving a blue ESR-active (19-plet, $g = 2.0489$, A = 52.5 G) species $[Nb_2(\mu\text{-}Se_2)_2(dtc)_4]^+$ at 638 mV *vs.* NHE. By contrast in the reaction of $[Nb_2(\mu\text{-}S_2)_2(acac)_4]$ **4** (Hacac = acetylacetone) with PEt_3Te only the sulfur abstraction product $[Nb_2(\mu\text{-}S)_2(acac)_4]$ **5** formed, which could be more directly prepared from **4** and PEt_3. Crystal structures of **4** and **5** were determined.

Introduction

During the last few years we have devoted a part of our synthetic efforts to niobium clusters with bridging chalcogen atoms in the cluster core, in particular those with a $Nb_2(\mu\text{-}S_2)_2$ core, including the preparation and structural characterization of the first niobium aqua-complex $[Nb_2(\mu\text{-}S_2)_2(H_2O)_8]^{4+}$.[1–3] The key stage in this chemistry is the transformation of easily accessible but very inert polymeric NbS_2Cl_2[5,6] into soluble salts $[Nb_2S_4(NCS)_8]^{4-}$ by reaction with molten KNCS at 180 °C.[1,4] The NCS ligand can be then either directly substituted by various 1,1′-dithioacid ligands like $^-S_2CNEt_2$ (dtc) yielding in that particular case the air-stable molecular complex $[Nb_2(\mu\text{-}S)_2(dtc)_4]$ **1**[1] or it can be destroyed by heating with concentrated HCl to give the aqua-complex, a convenient material for preparation of other $Nb_2(\mu\text{-}S_2)_2$ complexes.[2,3] When $NbSe_2Cl_2$ reacts with KNCS under similar conditions, chalcogen scrambling gives the whole spectrum of possible species $Nb_2S_xSe_{4-x}$.[7,8] The same reaction proceeds cleanly between the solids in a vibration mill to give $K_4[Nb_2Se_4(NCS)_8]$, from which $[Nb_2Se_4\{S_2P(OR)_2\}_4]$ and $[Nb_2Se_4(S_2COR)_4]$ (R = Et or Pr^i) complexes were prepared.[9a] A disadvantage of this approach is the necessity to use rather exotic for most laboratories, though constructively simple, equipment.[9] We report here chalcogen substitution reactions in the $Nb_2(\mu\text{-}S_2)_2$ core with PEt_3Y (Y = Se or Te) as chalcogen-transfer reagents as a new synthetic approach to Nb/Se and Nb/Te clusters.

Experimental

Starting materials

The compounds $[Nb_2(\mu\text{-}S_2)_2(dtc)_4]$ **1**, $[Nb_2(\mu\text{-}S_2)_2(acac)_4]$ **4** and PEt_3Te were prepared by procedures described in the literature;[1,3,10] PEt_3Se was prepared by treating PEt_3 (20% w/w toluene solution) with amorphous selenium powder in toluene at room temperature. All solvents were purified by standard methods and degassed before use. Standard Schlenk techniques were used throughout the preparation and isolation of selenium and tellurium derivatives, though **2**, once prepared, is stable enough to be manipulated in air.

Preparations

$[Nb_2(\mu\text{-}Se_2)_2(dtc)_4]$ 2. To a solution of complex **1** (0.20 g, 0.22 mmol) in 10 ml CH_2Cl_2 was added solid PEt_3Se (0.38 g, 1.3 mmol) followed by 0.15 ml of a toluene solution of PEt_3 (20% w/w). The solution immediately turned golden-brown. After 1 h stirring at room temperature, the solution was evaporated to dryness, the solid washed with diethyl ether and dissolved in a small amount of $CHCl_3$. Ethanol was then carefully layered on the top of the solution to produce dark brown crystals after standing overnight (**2**·$2CHCl_3$). They easily lose solvent chloroform in air (within minutes) to give solvent-free **2**. The elemental analysis refers to the unsolvated product (Found: C, 21.8; N, 5.0; H, 3.8; S, 23.0. Calc. for $C_{10}H_{20}N_2NbS_4Se_2$: C, 21.9; N, 5.1; H, 3.7; S, 23.4%). Yield 0.15 g (65%). UV/VIS ($CHCl_3$, 300–1400 nm): 355 (sh), 412 and 615 (sh) nm. CV (THF, 0.1 M Bu_4NClO_4, *vs.* NHE, mV): −510 (reduction, irreversible), −78 (reduction, irreversible), 638 (quasireversible) and 1188 (oxidation, irreversible). IR (KBr, 4000–250 cm^{-1}): 270s, 365w, 400w, 575w, 780w, 815w, 875w, 915w, 1005m, 1080s, 1090 (sh), 1100 (sh), 1150s, 1195w, 1215s, 1305m, 1360s, 1380s, 1435s, 1460s, 1495s and 1540m. FAB-MS: *m/z* 1095 (3.9, $[M - H]^+$), 1063 (25.5, $[M - SH]^+$), 1015 (28.6, $[M - SeH]^+$) and 867 (11.0%, $[M - SeH - dtc]^+$). ^1H NMR ($CDCl_3$): δ 3.77 (2 H, center of broad multiplet), 1.32, 1.24 and 1.21 (m, 3 H).

$[Nb_2(\mu\text{-}S)(\mu\text{-}Te_2)(dtc)_4]$ 3. To a solution of complex **1** (0.16 g, 0.18 mmol) in 10 ml $CHCl_3$ solid PEt_3Te (0.19 g, 0.8 mmol) was added. The solution turned dark-brown immediately upon the PEt_3Te addition and some Te precipitated. After 3 h stirring at room temperature, the solution was evaporated to dryness, the solid was washed with ether (2 × 10 ml) and extracted with 5 ml CH_2Cl_2. The golden-brown solution was filtered and on the top of the filtrate diethyl ether (10 ml) was carefully layered to produce dark brown crystals after standing overnight

Table 1 Summary of crystallographic data for complexes **1**–**5**

	1	**2**·2CHCl$_3$	**3**·CHCl$_3$	**4**	**5**·CH$_2$Cl$_2$
Empirical formula	$C_{20}H_{40}N_4Nb_2S_{12}$	$C_{20}H_{40}N_4Nb_2S_8Se_4\cdot 2CHCl_3$	$C_{20}H_{40}N_4Nb_2S_9Te_2\cdot CHCl_3$	$C_{20}H_{28}Nb_2O_8S_4$	$C_{20}H_{28}Nb_2O_8S_2\cdot 2CH_2Cl_2$
M	907.10	1333.45	1185.49	710.49	816.23
T/K	296	296	173	293	173
Crystal system	Monoclinic	Monoclinic	Triclinic	Monoclinic	Triclinic
Space group	$C2/c$	$P2_1/n$	$P\bar{1}$	$C2/c$	$P\bar{1}$
a/Å	24.010(3)	10.899(5)	13.030(3)	23.923(3)	9.00(1)
b/Å	6.957(4)	12.42(1)	14.391(5)	7.868(3)	11.15(3)
c/Å	21.172(2)	17.406(5)	12.053(4)	17.819(3)	8.868(6)
α/°			97.61(3)		101.5(1)
β/°	94.460(9)	104.25(3)	110.81(2)	121.036(8)	95.69(10)
γ/°			78.40(3)		73.3(2)
U/Å^3	3526(1)	2282(2)	2064(1)	2873(1)	834(2)
Z	4	2	2	4	1
D_c/g cm^{-3}	1.710	1.940	1.907	1.642	1.625
μ/cm^{-1}	13.81	44.31	26.10	11.27	11.70
Diffractometer	Rigaku AFC5R	Rigaku AFC5R	Rigaku AFC7R	Rigaku AFC5R	Rigaku AFC7R
$2\theta_{max}$/°	55.0	60.0	55.1	55.0	44.9
No. reflections (total)	4479	7261	9893	3634	967
unique	4372	6934	9476	3547	798
observed [$I > 2\sigma(I)$]	2550	2981	3191	1917	784
No. variables	172	208	245	210	77
Structure solution	DIRDIF 92 PATTY[11]	SIR 92[12]	SIR 92	DIRDIF 92 PATTY	SIR 92
R	0.042	0.079	0.091	0.040	0.074
R'	0.027	0.049	0.055	0.024	0.078

(**3**·CHCl$_3$). They easily lose the solvent to give unsolvated **3**. The elemental analysis refers to the unsolvated product (Found: C, 22.8; N, 5.3; H, 3.8; S, 23.0. Calc. for $C_{20}H_{40}N_4Nb_2S_9Te_2$: C, 22.5; N, 5.3; H, 3.8; S, 23.4%). Yield 0.11 g (58%). UV/VIS (CHCl$_3$, 300–1400 nm): 369 and 785 nm. CV (THF, 0.1 M Bu_4NClO_4, *vs.* NHE, mV): 674 (oxidation, irreversible), 1100 (oxidation, irreversible), 900 (reduction, irreversible), 440 (reduction, irreversible) and −110 (reduction, irreversible).

[Nb$_2$(μ-S$_2$)$_2$(dtc)$_4$]PF$_6$ 1a and [Nb$_2$(μ-Se$_2$)$_2$(dtc)$_4$]PF$_6$ 2a. A mixture of complex **2** (0.1 g, 0.09 mmol) and [FeCp$_2$]PF$_6$ (0.03 g, 0.09 mmol) was stirred in methylene chloride for 1 h. On the top of the resulting blue solution a double volume of hexane was layered. After standing for 2 d at −20 °C, 72 mg of crystalline **2a** were isolated as long needles. Yield 64% (Found: C, 21.0; H, 3.5; N, 4.3. Calc. for $C_{20}H_{40}F_6N_4Nb_2PS_8Se_4$: C, 19.4; H, 3.3; N, 4.5%). IR (KBr, 4000–250 cm^{-1}): 378m, 565s, 778w, 840vs, (PF$_6$), 900w, 1000w, 1075m, 1090w, 1150m, 1205s, 1272s, 1300w, 1355s, 1375m, 1439s, 1456s, 1517s, 2867w, 2922m and 2955m. UV/VIS in CH$_2$Cl$_2$ (λ/nm; ε/M^{-1} cm^{-1}): 675 (sh) (5200), 598 (8150) and 397 (5300). ESR (CH$_2$Cl$_2$, 293 K): $g = 2.0489$, $A = 52.5$ G.

Complex **1a** was prepared and isolated (as a blue-violet powder) similarly except that three times the stoichiometric amount of oxidant was used owing to the less favourable oxidation potential of **1** compared to **2** (Found: C, 22.5; H, 3.7; N, 4.9. Calc. for $C_{20}H_{40}F_6N_4Nb_2PS_{12}$: C, 22.8; H, 3.8; N, 4.9%). IR (KBr, 4000–250 cm^{-1}): 285m, 375m, 560s, 780w, 840vs, 915w, 1000m, 1075m, 1090m, 1145m, 1205m, 1275s, 1300m, 1355s, 1380m, 1450s, 1460m, 1505 (sh) and 1515s. UV/VIS in CH$_2$Cl$_2$ (λ/nm): 592, 518 (sh) and 364; ε values were not quantified due to instability of the solutions. The ESR spectrum is reported elsewhere.[1]

[Nb$_2$(μ-S)$_2$(acac)$_4$] 5. To a red solution of [Nb$_2$(μ-S$_2$)$_2$(acac)$_4$] **4** (0.18 g, 0.25 mmol) in 10 ml CH$_2$Cl$_2$ solid PEt$_3$Te (0.38 g, 1.56 mmol) was added, causing immediate darkening and precipitation of elemental Te. The mixture was left stirring overnight, then filtered and the filtrate reduced to 2 ml. After keeping for 1 h at −20 °C, 0.12 g of dark green crystalline **5** was collected. Yield 75% (Found: C, 37.8; H, 5.0; S, 8.9. Calc. for $C_{10}H_{14}NbO_4S$: C, 37.2; H, 4.4; N, 9.9%).

Crystallography

A summary of the crystal data, data collection and structure solution details is given in Table 1. Crystals of complexes **1** and **4** were mounted in air on a glass fiber, those of **2**·2CHCl$_3$ in a capillary together with a drop of mother-liquor and sealed in air. Crystals of **3**·CHCl$_3$ and **5**·2CH$_2$Cl$_2$ were picked up from the mother-liquor, immersed in glue under N$_2$, fixed on a glass fiber and immediately cooled to 173 K. Unit cell dimensions were determined and refined from 25 reflections in the 2θ ranges (°) 24.34–32.46 for **1**, 23.54–35.09 for **2**·2CHCl$_3$, 29.71–29.97 for **3**·CHCl$_3$ and 21.21–27.51 for **4**. For **5**·2CH$_2$Cl$_2$, 14 reflections in the range 7.61–15.87° were used to determine the cell. Intensity data were collected with the ω–2θ scan mode using graphite-monochromated Mo-Kα radiation (λ 0.71069 Å). In the case of **2** a 10.4% decrease in the intensity of standards over the course of data collection was observed and the intensity data were linearly corrected.

The structures were solved by the Patterson method (**1** and **4**) or by the direct method (**2**·2CHCl$_3$, **3**·CHCl$_3$ and **5**·2CH$_2$Cl$_2$) and expanded using Fourier techniques. The reflections were empirically corrected for absorption by the program DIFABS[13] after all non-hydrogen atoms were isotropically refined. Finally the structures were refined by the full-matrix least-squares method. In **1**, **2**·2CHCl$_3$, and **4**, all non-hydrogen atoms were anisotropically refined. In **3**·CHCl$_3$, only heavy atoms (Nb, S, Te and Cl) were anisotropically treated, other non-hydrogen atoms being refined isotropically. Hydrogen atoms were located in the calculated positions in **1**, **2**·2CHCl$_3$, **3**·3CHCl$_3$, while they were isotropically refined in **4**.

The data collection of complex **5**·2CH$_2$Cl$_2$ had to be discontinued due to trouble with the diffractometer. Since the crystals became amorphous quickly by losing solvent molecules the measurement of reflection intensities could not be continued. Therefore, the structure was determined based on a partial set of reflections. All non-hydrogen atoms were isotropically refined and hydrogen atoms were not included in the calculation. We report the structure to show the non-quantitative geometry of complex **5**.

The structure of [Nb$_2$S$_4$(Et$_2$NCS$_2$)$_4$] **1′** reported previously[14] appeared to be disordered. We employed a different solvent system to grow single crystals of **1** (CH$_3$CN–CH$_2$Cl$_2$ instead of CH$_2$Cl$_2$–hexane). The cell constants of **1′** [$a = 21.181(8)$,

$b = 6.958(1)$, $c = 16.623(6)$ Å, $\beta = 133.95°$, $V = 1764(2)$ Å^3, space group $C2/m$, $Z = 2$] are different from those of **1** but are convertible into them by the following transformation: $a' = a + 2c$, $b' = -b$, $c' = a$. The cell volume of the converted cell is $V' = 3528$ Å^3 and the resulting lattice is also *C*-centered. No disorder was found in **1**. It is possible that **1** and **1′** are genuine polymorphs (ordered and disordered) or **1′** may be the same as **1** but only its subcell was determined.

For the acac complex **4** cell parameters have been reported (space group *C*2) but the structure could not be refined.[3] We have finally solved the structure in the *C*2/*c* space group.

CCDC reference number 186/1238.

See http://www.rsc.org/suppdata/dt/1999/85/ for crystallographic files in .cif format.

Results and discussion

Chalcogen substitution reactions

In the early 90s we suggested PPh_3Se and KNCSe as effective chalcogen-transfer reagents for introduction of Se into the $[Mo_3(\mu\text{-}S)(\mu\text{-}S_2)_3]^{4+}$ cluster core to give a $[Mo_3(\mu\text{-}S)(\mu\text{-}SSe)_3]^{4+}$ core with novel SSe ligands.[15] Ibers and co-workers found that Se in polyselenido complexes can be substituted by using PEt_3Te instead of the non-existent PPh_3Te. This works for polyselenido complexes of Ni, Pt,[16] Zn, Cd and Hg.[17] We found, however, that **1** does not react with pure PEt_3Se, whereas adding small amounts of free PEt_3 to the mixture immediately brings about a colour change and gives **2** as the sole product. No mixed S/Se species were observed in this case. The necessity of adding free PEt_3 suggests that the reaction proceeds *via* initial abstraction of S from S_2 by phosphine giving a Nb(μ-S)-(μ-S_2)Nb unit. The bridging monosulfide ligand thus produced is nucleophilic enough to abstract Se from PEt_3Se thus forming a SSe unit and regenerating free phosphine. The reaction proceeds further with repeating cycles of sulfur abstraction/selenium insertion up to the final product, **2**. The P=S bond is energetically preferable over P=Se, and phosphines attack S–S bonds much faster (orders of magnitude!) than Se–Se bonds.[18] The same observations are valid for PMe_2PhSe, which also gives **2**. In the case of PEt_3Te there is always some free phosphine present in the solution as a result of partial dissociation into PEt_3 and Te, thus enabling the substitution to proceed without an extra PEt_3 source.[10]

Complex **3** is a rare example (and the first for Nb) of a cluster having both Te and S in the cluster core. As for its formation in place of the expected $Nb_2(Te_2)_2$ derivative, two comments may be relevant. First, chalcogen substitution reactions with PEt_3Te often proceed beyond simple substitution and may involve dramatic changes in structure.[16] Secondly, the $Nb_2(Te_2)_2$ core is known in $[Nb_2(Te_2)_2][Te_2I_6]_2$, prepared by high temperature reaction from the elements and thus thermodynamically stable.[19] With **4**, where dtc ligands are replaced by acac, the reaction with PEt_3Te takes another course leading to sulfur abstraction only with the formation of the bis(monosulfido) bridged **5**. As acac is more electronegative than dtc, the nucleophilicity of bridging sulfur in **5** is probably not high enough to form an intermediate with a S–Te bridge. The use of PEt_3 instead of PEt_3Te in the reaction with **4** gives the same complex **5** in a more straightforward manner. Sulfur abstraction by PPh_3 was used before to prepare $[Nb_2(\mu\text{-}S)_2Cl_4(tht)_4]$ from $[Nb_2(\mu\text{-}S)(\mu\text{-}S_2)Cl_4(tht)_4]$ (tht = tetrahydrothiophene), where the reaction time was 3 months at 50 °C.[20] Another approach to $Nb_2S_2^{4+}$ involves methathesis of $NbCl_4L_2$ with Sb_2S_3 or $(Me_3Si)_2S$ (L = MeCN or THF).[21,22]

Molecular complexes with the $[Nb_2(\mu\text{-}Se_2)_2]^{4+}$ core were first prepared by treating $NbSeCl_3$ (structure unknown) with thioesters. The products thus prepared were $[Nb_2Se_4Cl_4(tht)_4]$ and $[Nb_2Se_4Cl_4(Me_2S)_4]$.[23,24] The compounds $NbSe_2X_2$ (X = Cl, Br or I) which contain $[Nb_2(\mu\text{-}Se_2)_2]^{4+}$ units linked by halide bridges into an infinite layer structure are far too inert within the ordinary range of reaction temperatures and solvents; $NbSe_2I_2$ reacts with Te and I_2 (effectively TeI_2) at 500 °C to give $[Nb_2(\mu\text{-}Se_2)_2][Te_2I_6]_2$ with $Te_2I_6^{2-}$ acting as a tetradentate ligand.[25] Taking the greater accessibility and stability of Nb_2S_4 derivatives into account, chalcogen substitution of Se for S suggests itself as a viable synthetic alternative for preparation of their Nb_2Se_4 analogs.

Oxidation of $[Nb_2(\mu\text{-}Y_2)_2(dtc)_4]$

Chemical oxidation of $[Nb_2(\mu\text{-}S_2)_2(dtc)_4]$ **1** by Fc^+ has been reported.[1] The one-electron oxidation product, cation-radical $\mathbf{1}^+$, was characterized in solution by ESR spectroscopy. We found that **2** is also oxidized by Fc^+ to give ESR active species $\mathbf{2}^+$. The ESR spectra of both $\mathbf{1}^+$ and $\mathbf{2}^+$ give a similar 19-plet pattern due to the hyperfine interaction of the single unpaired d electron with the two ^{93}Nb nuclei. The *A* and *g* parameters are similar for $\mathbf{1}^+$ and $\mathbf{2}^+$ (*A*: $\mathbf{1}^+$, 54.0; $\mathbf{2}^+$, 52.5 G: *g*: $\mathbf{1}^+$, 2.0113; $\mathbf{2}^+$, 2.0489). They differ from those expected for a simple d^1 system which probably reflects a contribution of the p orbitals of the bridging dichalcogen units and/or of the dtc ligands.[1] The solutions of $\mathbf{1}^+$ are not stable and decompose at room temperature within 2–3 d into unidentified products; $\mathbf{2}^+$ is more stable in solutions. Solid samples of [**1**]PF_6 and [**2**]PF_6 have also been prepared. Similarly, the BF_4 and BPh_4 salts were also isolated. Our efforts to obtain good quality single crystals have failed so far.

Cyclic voltammetry studies

Cyclic voltammetry was performed for complexes **1**, **2** and **3** in THF in the presence of 0.1 M Bu_4NClO_4. Complexes **1** and **2** show similar quasireversible waves at 770 (**1**) and 638 mV (**2**) *vs.* NHE which can be attributed to a one electron oxidation identical with that effected by Fc^+. For both cases $I_c = I_a$ but ΔE for **1** was 294 mV, for **2** 207 mV. This can be explained by changes in geometry of the complexes after oxidation, primarily because one would expect elongation of the Nb–Nb bond as one d electron is removed and the formal bond order is thus reduced to 0.5. The second oxidation is irreversible and takes place at rather high positive potentials, about 1600 mV for **1** and 1188 mV for **2**. No reversible reduction behaviour was found for **1** and **2** (and for **3** and **4** as well). It is interesting that the disulfide bridged cluster **1** is oxidized at about 130 mV more positive potential than is **2**.

Crystal structures

The complexes **1**, **2**, **4** and **5** all have an inversion center at the midpoint of the bonded Nb atoms; **3** has no crystallographic symmetry but has a pseudomirror plane perpendicular to the Nb–Nb bond.

Nb_2S_4 clusters. Views of $[Nb_2S_4(dtc)_4]$ **1** and $[Nb_2S_4(acac)_4]$ **4** are shown in Figs. 1 and 2, respectively. Bond distances are given in Tables 2 and 3. The parameters of the Nb_2S_4 core vary only slightly with the change of other "external" ligands at Nb.[1–3,5,6,14] In agreement with this, a typical S–S distance of 2.033(2) Å was found in **1**, instead of the previously reported value 2.282(5) Å for **1′**.[14] The Nb–Nb distances in all known $Nb_2S_4^{4+}$ clusters fall within the 2.86–2.91 Å range which is longer than 2.81–2.86 Å for isoelectronic $Mo_2S_4^{6+}$ clusters and might reflect a weaker Nb–Nb bonding, but it does not necessarily mean greater stability of the Mo_2S_4 species. Indeed we found that the latter are prone to transform internally under conditions where their niobium counterparts are stable.[2,26] It is also interesting to compare the geometries of the acac complex **4** and of $[Nb_2S_4(tfa)_4]$ [tfa represents O,O′ co-ordinating $CF_3C(O)CHC(O)CH_3$ ligand].[3] In the latter the Nb_2S_4 core is "compressed" as compared with **4** [Nb–Nb 2.879(1) *vs.*

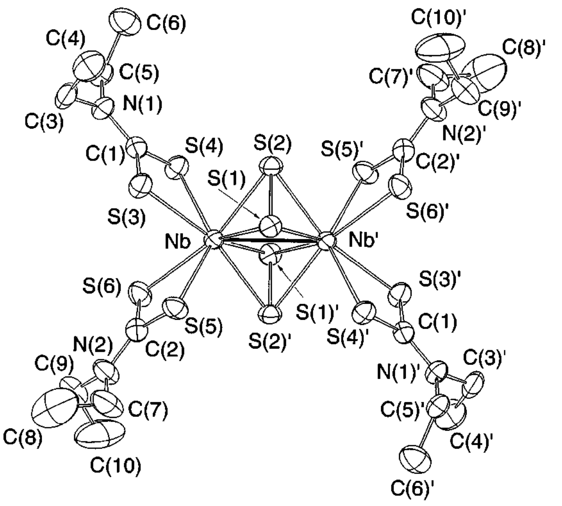

Fig. 1 View of the structure of $[Nb_2S_4(Et_2NCS_2)_4]$ **1**.

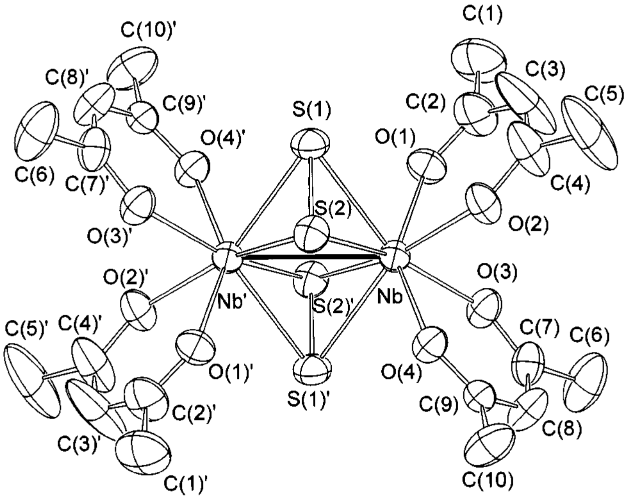

Fig. 2 View of the structure of $[Nb_2S_4(acac)_4]$ **4**.

Table 2 Selected bond lengths (Å) in complex **1**

Nb–Nb	2.8928(9)	Nb–S(1)	2.520(1)
Nb–S(2)	2.492(1)	Nb–S(3)	2.598(2)
Nb–S(4)	2.586(1)	Nb–S(5)	2.569(2)
Nb–S(6)	2.619(2)	S(1)–S(2)	2.033(2)
S(3)–C(1)	1.727(5)	S(4)–C(1)	1.708(5)
S(5)–C(2)	1.705(6)	S(6)–C(2)	1.723(6)
N(1)–C(1)	1.325(5)	N(1)–C(3)	1.472(7)
N(1)–C(5)	1.471(6)	N(2)–C(2)	1.324(6)
N(2)–C(7)	1.468(8)	N(2)–C(9)	1.463(7)
C(3)–C(4)	1.492(8)	C(5)–C(6)	1.508(7)
C(7)–C(8)	1.477(9)	C(9)–C(10)	1.500(8)

Table 3 Selected bond lengths (Å) in complex **4**

Nb–Nb	2.9039(9)	Nb–S(1)	2.535(1)
Nb–S(1)	2.534(1)	Nb–S(2)	2.498(1)
Nb–S(2)	2.508(2)	Nb–O(1)	2.147(4)
Nb–O(2)	2.127(4)	Nb–O(3)	2.131(3)
Nb–O(4)	2.143(3)	S(1)–S(2)	2.019(2)
O(1)–C(2)	1.245(6)	O(2)–C(4)	1.250(7)
O(3)–C(7)	1.252(6)	O(4)–C(9)	1.245(5)
C(1)–C(2)	1.506(10)	C(2)–C(3)	1.394(9)
C(3)–C(4)	1.39(1)	C(4)–C(5)	1.51(1)
C(6)–C(7)	1.508(9)	C(7)–C(8)	1.398(9)
C(8)–C(9)	1.400(7)	C(9)–C(10)	1.487(9)

2.9039(9) in **4**; S–S 2.008(4) *vs.* 2.019(2) and Nb–S (average) 2.504 *vs.* 2.519 Å]. This may be simply due to the higher electronegativity of the fluorinated ligand, which reduces the electron density (and effective radius) at Nb and thus enhances the donation from S_2 π^* to niobium d_π orbitals.

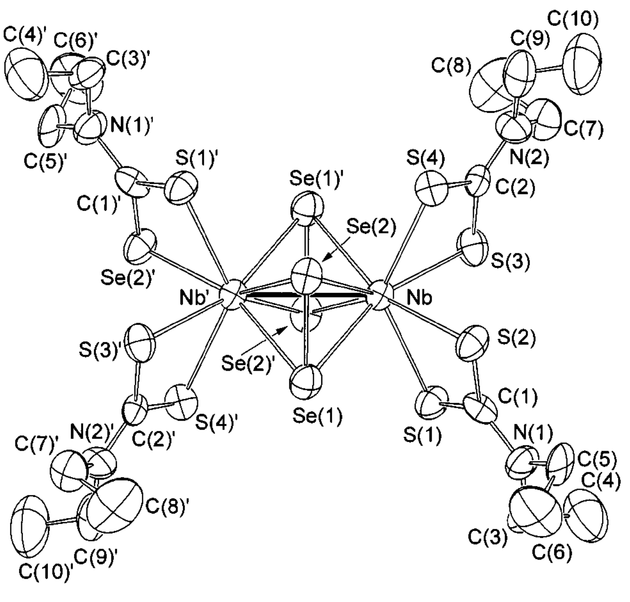

Fig. 3 View of the structure of $[Nb_2Se_4(Et_2NCS_2)_4]$ **2**.

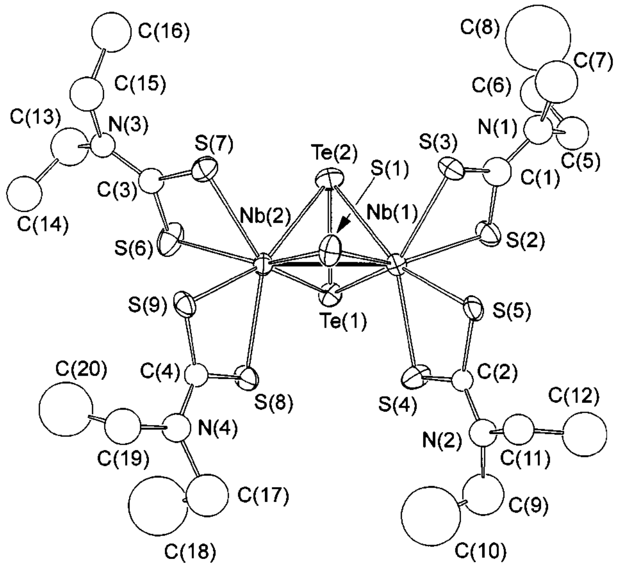

Fig. 4 View of the structure of $[Nb_2(S)(Te_2)(Et_2NCS_2)_4]$ **3**.

Table 4 Selected bond lengths (Å) in complex **2**

Nb–Nb	2.974(2)	Nb–Se(1)	2.639(2)
Nb–Se(1)	2.625(2)	Nb–Se(2)	2.644(2)
Nb–Se(2)	2.649(2)	Nb–S(1)	2.585(3)
Nb–S(2)	2.607(4)	Nb–S(3)	2.609(4)
Nb–S(4)	2.593(4)	Se(1)–Se(2)	2.303(2)
Cl(1)–C(11)	1.67(1)	Cl(2)–C(11)	1.65(1)
Cl(3)–C(11)	1.76(2)	S(1)–C(1)	1.73(1)
S(2)–C(1)	1.68(1)	S(3)–C(2)	1.68(1)
S(4)–C(2)	1.73(1)	N(1)–C(1)	1.40(1)
N(1)–C(3)	1.45(2)	N(1)–C(5)	1.45(1)
N(2)–C(2)	1.34(1)	N(2)–C(7)	1.46(2)
N(2)–C(9)	1.43(2)	C(3)–C(4)	1.47(2)
C(5)–C(6)	1.45(2)	C(7)–C(8)	1.48(2)
C(9)–C(10)	1.42(2)		

Nb_2Se_4 core. The Nb–Nb bonds are further elongated when Se is substituted for S (Fig. 3, Table 4). The Nb–Nb distance found in **2**, 2.974(2) Å, is close to those observed in $[Nb_2Se_4][Te_2I_6]_2$ [2.926(2) Å],[25] $[Nb_2Se_4Cl_4(Me_2S)_4]$ [2.962(3) Å], $[Nb_2Se_4Cl_4(tht)_4]$ [2.972(5) Å][20,23] and in polymeric $NbSe_2Cl_2$ [2.973(4) Å].[27] The Se–Se distance [2.303(2) Å] is longer than in

Table 5 Selected bond lengths (Å) in complex **3**

Te(1)–Te(2)	2.648(3)	Te(1)–Nb(1)	2.844(3)
Te(1)–Nb(2)	2.854(3)	Te(2)–Nb(1)	2.848(3)
Te(2)–Nb(2)	2.842(3)	Nb(1)–Nb(2)	2.920(4)
Nb(1)–S(1)	2.376(7)	Nb(1)–S(2)	2.625(8)
Nb(1)–S(3)	2.581(8)	Nb(1)–S(4)	2.499(7)
Nb(1)–S(5)	2.618(7)	Nb(2)–S(1)	2.387(8)
Nb(2)–S(6)	2.581(8)	Nb(2)–S(7)	2.581(7)
Nb(2)–S(8)	2.511(7)	Nb(2)–S(9)	2.593(8)
Cl(1)–C(21)	1.33(6)	Cl(2)–C(21)	1.78(6)
Cl(3)–C(21)	2.01(5)	S(2)–C(1)	1.69(3)
S(3)–C(1)	1.73(3)	S(4)–C(2)	1.75(2)
S(5)–C(2)	1.70(2)	S(6)–C(3)	1.71(2)
S(7)–C(3)	1.74(3)	S(8)–C(4)	1.72(2)
S(9)–C(4)	1.67(2)	N(1)–C(1)	1.32(3)
N(1)–C(5)	1.51(3)	N(1)–C(7)	1.62(4)
N(2)–C(2)	1.33(3)	N(2)–C(9)	1.58(4)
N(2)–C(11)	1.43(3)	N(3)–C(3)	1.33(3)
N(3)–C(13)	1.50(4)	N(3)–C(15)	1.55(3)
N(4)–C(4)	1.33(3)	N(4)–C(17)	1.64(4)
N(4)–C(19)	1.65(4)	C(5)–C(6)	1.52(4)
C(7)–C(8)	1.24(8)	C(9)–C(10)	1.40(7)
C(11)–C(12)	1.50(5)	C(13)–C(14)	1.51(4)
C(15)–C(16)	1.55(4)	C(17)–C(18)	1.24(8)
C(19)–C(20)	1.45(6)		

both Me_2S [2.288(3) Å] and tht [2.260(5) Å] complexes,[20,23] but somewhat shorter than in the complex with $Te_2I_6^{2-}$ ligands [2.310–2.311(2) Å].[25] The average Nb–S (dtc) distances are almost identical for **1** and **2**, being 2.593 Å in the former and 2.598 Å in the latter compound.

Nb_2STe_2 core. Cluster **3** has a unique $Nb_2(S)(Te_2)^{4+}$ core (Fig. 4, Table 5). The Te_2 ligand is co-ordinated unsymmetrically with one Te atom in the Nb_2S plane and the other out of the plane. The Nb–Te distances are however almost identical [Nb–Te(1) 2.844(3)–2.854(3), Nb–Te(2) 2.842(3)–2.848(3) Å]. In $[Nb_2(\mu\text{-}S)(\mu\text{-}S_2)X_4(tht)_3]$ (X = Cl or Br) the S_2 ligand adopts a more symmetrical co-ordination with the two Nb atoms, bridging S atom and the midpoint of the S_2 unit being almost coplanar.[28] The Te–Te distance, 2.648(3) Å, is close to that observed in $[Nb_2(Te_2)_2][Te_2I_6]_2$ [2.682(1) Å], the only $Nb_2(Te_2)_2^{4+}$ cluster so far known. The Nb–Nb distance in the latter is however much longer than in **3** [3.083(2) *vs.* 2.920(4) Å].[19] As calculations show that the potential minimum for Nb–Nb interaction is rather flat between 2.9 and 3.1 Å,[19] the continuous elongation of the Nb–Nb distance on going from Nb_2S_4 *via* Nb_2Se_4 to Nb_2Te_4 is caused by the necessity to accommodate two larger dichalcogenido groups, keeping the van der Waals repulsion between them minimal. The steric requirements of one S and one Te_2 group are more modest compared to those of two Te_2 ligands, thus allowing two Nb atoms to be almost as close as they are in Nb_2S_4 clusters.

Et_2NCS_2 ligands. In the complexes **1**, **2** and **3** the dtc ligands have their usual geometry where a nitrogen atom, two sulfur atoms, and 3 carbon atoms are coplanar. The two terminal CH_3 groups may be either *cis* or *trans* with regard to this plane. In the case of **1** each Nb has one of each sort (Fig. 1) and in the case of **2** they are all *trans* (Fig. 3). Again, **3** has one of each kind similarly to **1** (Fig. 4). It is unlikely that the energy differences between *cis* and *trans* forms are large and the configuration in the crystal is dictated mainly by the packing forces.

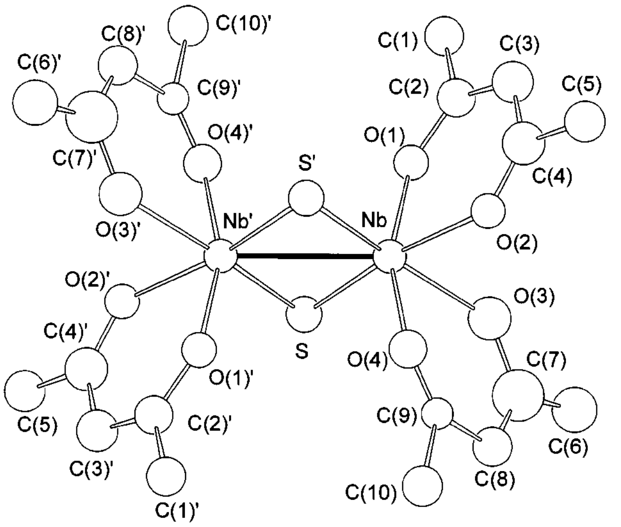

Fig. 5 View of the structure of $[Nb_2S_2(acac)_4]$ **5**.

Table 6 Selected bond lengths (Å) in complex **5**

Nb–Nb	2.880(5)	Nb–S	2.393(7)
Nb–S	2.37(1)	Nb–O(1)	1.99(1)
Nb–O(2)	2.15(1)	Nb–O(3)	2.29(3)
Nb–O(4)	1.98(2)	Cl(1)–C(11)	1.75(3)
Cl(2)–C(11)	1.75(4)	O(1)–C(2)	1.35(3)
O(2)–C(4)	1.30(3)	O(3)–C(7)	1.39(5)
O(4)–C(9)	1.22(5)	C(1)–C(2)	1.57(3)
C(2)–C(3)	1.42(2)	C(3)–C(4)	1.47(3)
C(4)–C(5)	1.57(3)	C(6)–C(7)	1.41(5)
C(7)–C(8)	1.45(3)	C(8)–C(9)	1.56(5)
C(9)–C(10)	1.64(3)		

Co-ordination around Nb. In terms of a formalism in which the niobium co-ordination in bis(dichalcogenido) bridged dimers **1**, **2** and **4** is described as pseudooctahedral by taking the midpoints of the Y_2 units to be the positions of imaginary monodentate ligands, each of these octahedra possesses chirality at the Nb. Using Λ and Δ designations, the observed configurations in the centrosymmetrical molecules of **1**, **2** and **4** are represented as ΛΔ, *i.e.* they all are *meso* isomers. Other such d^1–d^1 dimers existing as *meso* forms are $[V_2S_4(Et_2NCS_2)_4]$, $[Mo_2S_4(Et_2NCS_2)_4][BF_4]_2$ and $[W_2S_4(Et_2NCS_2)_4]I[I_3]$.[29,30] An equilibrium between *meso* ΛΔ and a racemic mixture of chiral ΛΛ + ΔΔ isomers may exist in solution. Indeed, the ^1H NMR spectrum of the acac complex **4** at room temperature (in $CDCl_3$) shows two well separated sharp singlets (at δ 5.55 and 5.52) for the proton attached to the central C atom of the acac ligand. This pattern arises from coexistence of the two isomers. In the case of $[V_2S_4(S_2CN^tBu_2)_4]$ it is the racemic mixture that crystallizes from solutions.[31] In **5** (Fig. 5, Table 6) the geometry around Nb is octahedral (2S + 4O′) and it also exists in the *meso* form in the crystal. Complex **3** has two independent Nb atoms. The co-ordination of Nb(1) may be described as distorted pentagonal bipyramidal with basal S(1), S(2), S(3), S(4) and Te(1) and apical S(5) and Te(2) atoms or as distorted monocapped octahedral with Te(2) capping the face formed by Te(1), S(3) and S(2). The co-ordination around Nb(2) is too distorted to be approximated as a simple polyhedron.

Acknowledgements

We thank the Japan Society for the Promotion of Science for granting a research fellowship to M. S. He is also thankful to the Institute of Inorganic Chemistry (Novosibirsk) for leave of absence. Thanks are also due to Dr. A. Virovets for helpful discussions.

References

1 M. Sokolov, A. Virovets, V. Nadolinnyi, K. Hegetschweiler, V. Fedin, N. Podberezskaya and V. Fedorov, *Inorg. Chem.*, 1994, **33**, 3503.
2 M. Sokolov, R. Hernandez-Molina, M. R. J. Elsegood, S. L. Heath, W. Clegg and A. G. Sykes, *J. Chem. Soc., Dalton Trans.*, 1997, 2059.

3 M. Sokolov, O. Geras'ko, A. Virovets and V. Fedorov, *Inorg. Chim. Acta*, 1998, **271**, 222.

4 A. Mishchenko, V. Fedorov, B. Kolesov and M. Fedotov, *Koord. Khim.*, 1989, **15**, 200.

5 W. Beckmann and H. Schäfer, *Z. Anorg. Allg. Chem.*, 1966, **347**, 225.

6 H.-G. von Schnering and W. Beckmann, *Z. Anorg. Allg. Chem.*, 1996, **347**, 231.

7 M. Sokolov, V. Fedin, K. Hegetschweiler, A. Müller and V. Fedorov, *Zh. Neorg. Khim.*, 1994, **39**, 1663.

8 A. Virovets, M. Sokolov, N. Podberezskaya and V. Fedorov, *Zh. Struct. Khim.*, 1996, **37**, 525.

9 (*a*) M. Sokolov, S. Tkachev, V. Fedorov and V. Fedin, *Zh. Neorg. Khim.*, 1996, **41**, 1124; (*b*) M. Sokolov, V. Fedin, K. Myakishev, O. Geras'ko, V. Fedorov and Y. Macichek, *Polyhedron*, 1991, **10**, 1311.

10 R. A. Zingaro, B. H. Steeves and K. Irgolic, *J. Organomet. Chem.*, 1965, **4**, 320.

11 P. T. Beurskens, G. Admiraal, G. Beurskens, W. P. Bosman, S. Garcia-Granda, R. O. Gould, J. M. M. Smits and C. Smykalla, DIRDIF 92, Technical Report of the Crystallographic Laboratory, University of Nijmegen, 1992.

12 A. Altomare, M. C. Burla, M. Camalli, M. Cascarano, C. Giacivazzo, A. Guagliardi and G. Polidori, SIR 92, *J. Appl. Crystallogr.*, 1994, **27**, 1045.

13 N. Walker and D. Stuart, DIFABS, *Acta Crystallogr., Sect. A*, 1983, **39**, 158.

14 A. V. Virovets, N. V. Podberezskaya, M. N. Sokolov, I. V. Korobkov, V. P. Fedin and V. Fedorov, *Zh. Struct. Khim.*, 1993, **34**, 134.

15 V. Fedin, Yu. Mironov, M. Sokolov, B. Kolesov, V. Fedorov, D. Yufit and Yu. Struchkov, *Inorg. Chim. Acta*, 1990, **174**, 275.

16 J. M. McConnachie, J. C. Bollinger and J. A. Ibers, *Inorg. Chem.*, 1993, **32**, 3923.

17 J. C. Bollinger and J. A. Ibers, *Inorg. Chem.*, 1995, **34**, 1859.

18 D. M. Saysell, V. P. Fedin, G. J. Lamprecht, M. N. Sokolov and A. G. Sykes, *Inorg. Chem.*, 1997, **36**, 2982.

19 A. Leist and W. Tremel, *Angew. Chem.*, 1993, **105**, 1798.

20 M. G. B. Drew, D. A. Rice and D. M. Williams, *J. Chem. Soc., Dalton Trans.*, 1985, 417.

21 M. Yoon, V. Young, Jr. and G. J. Miller, *Acta Crystallogr., Sect. C*, 1997, **53**, 1041.

22 A. J. Benton, M. G. B. Drew, R. J. Hobson and D. A. Rice, *J. Chem. Soc., Dalton Trans.*, 1981, 1304.

23 M. G. B. Drew, D. A. Rice and D. M. Williams, *J. Chem. Soc., Dalton Trans.*, 1984, 1087.

24 M. G. B. Drew, D. A. Rice and D. M. Williams, *Acta Crystallogr., Sect. C*, 1984, **40**, 1547.

25 V. P. Fedin, V. Fedorov, H. Imoto and T. Saito, *Polyhedron*, 1997, **16**, 995.

26 M. N. Sokolov, O. A. Geras'ko and V. E. Fedorov, *Zh. Neorg. Khim.*, 1998, **43**, 407.

27 J. Rijnsdorp, G. J. de Lange and G. A. Wiegers, *J. Solid State Chem.*, 1979, **30**, 365.

28 M. G. B. Drew, D. A. Rice and D. M. Williams, *J. Chem. Soc., Dalton Trans.*, 1983, 2251.

29 E. R. T. Tiekink, X. F. Yan and C. G. Young, *Aust. J. Chem.*, 1992, **45**, 897; Y. Yang, L. Huang, Q. Liu and B. Kang, *Acta Crystallogr., Sect. C*, 1991, **47**, 2085.

30 C. G. Young, T. O. Kocaba, X. F. Fan, E. R. T. Tiekink, L. Wei, H. H. Murray III, C. L. Coyle and E. I. Stiefel, *Inorg. Chem.*, 1994, **33**, 6252.

31 T. R. Halbert, L. L. Hutchings, R. Rhodes and E. I. Stiefel, *J. Am. Chem. Soc.*, 1986, **108**, 6437.

Paper 8/06627B